

Mixed Eccentricity Fault Diagnosis in Saturated Squirrel Cage Induction Motor using Instantaneous Power Spectrum Analysis

Abstract. Mixed eccentricity fault is one of the most common faults occurring in squirrel cage induction motors. Several techniques have been used to detect this type of fault, such as those based on vibration, axial leakage monitoring, zero-sequence component, negative sequence current, and motor current signature analysis. However, these techniques do not take into account the effect of magnetic saturation. In this paper, Instantaneous Power Signature Analysis (IPS) technique is used to detect this kind of fault, it shows the effect of harmonic saturation on the mixed eccentricity fault diagnosis of squirrel induction motors. Both simulation and experimental results for healthy and faulty motors are shown and discussed.

Streszczenie. Do analizy ekscentryczności silnika indukcyjnego powszechnie używa się monitorowania wibracji, rozproszenia osiowego, negatywnej sekwencji prądu i kształtu prądu. Metody te niestety nie biorą pod uwagę nasycenia magnetycznego. W artykule zaproponowano metodę IPS (analiza sygnatury prądu) analizująca nasycenie harmonicznych. Przedstawiono wyniki symulacji i eksperymentalne metody. Diagnostyka Ekscentryczności w nasyconym silniku indukcyjnym metodą badania spektrum mocy.

Keywords: Eccentricity Fault Diagnosis, Saturated, Instantaneous power Spectrum, squirrel cage induction motor.

Słowa kluczowe: ekscentryczność silnika indukcyjnego, analiza spectrum mocy.

Introduction

The Squirrel cage induction motors (SCIM) are widely used in many industrial applications, because they are characterized by high reliability, low cost per power unit, high power per volume unit and need very low maintenance. Although these are very reliable, they are subjected to different modes of failures faults. These faults may be inherent to the machine itself or due to the operating conditions. The inherent faults may be due to the mechanical or electrical forces acting on the machine enclosure. A variety of machine faults are studied in the literature [1, 2, 3], such as winding faults, unbalanced stator and rotor parameters, broken rotor bars, eccentricity and bearing faults. Several fault identification method have been developed and been effectively applied to detect machine faults at different stages by using different machine parameters, such as current, voltage, speed, efficiency, temperature and vibrations. A diagnosis technique which can detect a failure and prevent the total damage of the motor is therefore of great importance [4, 5, 6].

In our paper [7], a state of art of various approaches used in the modelling of the saturated induction motor, are presented. Also, in [7] a mathematical model based on of the modified winding function approach is developed, for the various inductances of SCIM calculating (taking into account both space harmonics of the magneto motive force and the magnetic saturation).

Simulation and the stator current spectral analysis, demonstrate at first, the importance of introducing the magnetic saturation in our model, which is reflected by the presence of harmonics, in the neighbourhood of the principal rotor slot harmonics (PSH) in the healthy motor, and secondly, for the faulty motor, the mixed eccentricity harmonics are in proximity of saturation harmonic position.

This paper introduces the application of instantaneous power spectrum analysis for diagnosis of the mixed air gap eccentricity, especially for the case of saturated squirrel cage induction motors (SSCIM).

The paper is organized as follows: Next section is focused on the presentation of the instantaneous power spectrum technique. In the third section, our results are presented, and validated.

The Saturated Squirrel Cage Induction Motor Model

Consider an SCIM having m stator circuits and n rotor bars. The cage can be viewed as n identical and equally

spaced rotor loops [2,7]. Voltage equations for the SCIM can be written in vector-matrix form as follows:

$$[V_s] = [R_s][I_s] + \frac{d[\Psi_s]}{dt} \quad (1)$$

$$[V_r] = [R_r][I_r] + \frac{d[\Psi_r]}{dt} \quad (2)$$

where

$$[V_s] = [v_1^s \ v_2^s \ \dots \ v_m^s]^T, [V_r] = [0 \ 0 \ \dots \ 0]^T \quad (3)$$

$$[I_s] = [i_1^s \ i_2^s \ \dots \ i_m^s]^T, [I_r] = [i_1^r \ i_2^r \ \dots \ i_n^r]^T \quad (4)$$

and the stator and rotor flux linkages are given by

$$[\Psi_s] = [L_{ss}][I_s] + [L_{sr}][I_r] \quad (5)$$

$$[\Psi_r] = [L_{rr}][I_r] + [L_{rs}][I_s] \quad (6)$$

L_{ss} is an $m \times m$ matrix with the stator self and mutual inductances, L_{rr} is an $n \times n$ matrix with the rotor self and mutual inductances, L_{sr} is an $m \times n$ matrix composed by the mutual inductances between the stator phases and the rotor loops, L_{rs} is an $n \times m$ matrix composed by the mutual inductances between the rotor loops and the stator phases and $L_{sr} = L_{rs}^t$.

The mechanical equations for the machine are

$$J \frac{d\omega_r}{dt} + T_L = T_e \quad (7)$$

$$\frac{d\theta_r}{dt} = \omega_r \quad (8)$$

where θ_r is the rotor position, ω is the angular speed, and is J the rotor-load inertia. T_L is the load torque. The machine

electromagnetic torque T_e can be obtained from the magnetic co-energy

$$(9) \quad T_e = \left[\frac{\partial W_{co}}{\partial \theta_r} \right]_{(I_s, I_r)}$$

The magnetic co-energy is the energy stored in the magnetic circuits and can be written as:

$$(10) \quad W_{co} = \frac{1}{2} [I_s' L_{ss} I_s + I_s' L_{sr} I_r + I_r' L_{rs} I_s + I_r' L_{rr} I_r]$$

All of the relevant inductances for the induction motor can be calculated using the MWFA given in [1,2]. According to the winding function theory, the mutual inductance between stator and rotor for SSCIM [] can be computed by:

$$(11) \quad L_{sr}(\theta) = 2\pi l \mu_0 \langle \delta n_s n_r \rangle - 2\pi l \mu_0 \frac{\langle \delta n_s \rangle \langle \delta n_r \rangle}{\langle \delta \rangle}$$

where r is the average radius of the air gap, l is the length of the stack, δ is the air gap permeance, n_s and n_r are the winding distribution of stator and rotor respectively, the permeance of saturated case can be defined as follow :

$$(12) \quad \delta(\phi, \theta) \approx \delta' [1 + k_{gsat} \cos\{2(p\phi - \theta)\}]$$

where, ϕ is the stator position, θ is the position of the air-gap flux, p is the number of pole pairs, δ' is average value of the air-gap and k_{gsat} is the saturation factor deduced from the hypothesis that the saturation effect amplifies the air-gap permeance at twice the frequency of the air-gap flux density wave. k_{gsat} has been obtained by the calculation of the ratio of the full load air gap voltage and no load air gap voltage.

Mixed Eccentricity Modelling

The air gap function for mixed eccentricity can be represented by,

$$(13) \quad \delta_s(\phi) = \delta_0 [1 - e_s \cos\phi - e_d \cos(\phi - \theta_r)]$$

where e_s and e_d are static and dynamic eccentricity amounts, respectively.

This equation is used in (11) for the SCIM self and mutual inductance calculation [7].

These inductances are functions of rotor positions and vary continuously along the air gap during mixed air gap eccentricity of the motor operation.

Instantaneous Power Signature Technique

We consider an ideal three-phase supply voltage. The instantaneous power $p(t)$, is defined as:

$$(14) \quad p(t) = v(t)i(t)$$

Where $v(t)$ is the voltage between any two of the three stator terminals and $i(t)$ is the terminal current input. The expression of the voltage $v(t)$, current $i(t)$ and instantaneous power are given by [6] :

$$(15) \quad v(t) = U_m \cos(2\pi ft)$$

$$(16) \quad i(t) = I_m \cos(2\pi ft - \varphi)$$

$$(17) \quad p(t) = \frac{U_m I_m}{2} \cos(2(2\pi f)t - \varphi) + \frac{U_m I_m}{2} \cos(\varphi)$$

where U_m and I_m are the amplitude of the supply voltage and current, respectively, f is the supply frequency, and φ is motor phase angle.

If the air gap eccentricity fault occurs in SCIM, the instantaneous power can be expressed as [8, 9, 10]:

$$p_{ecc}(t) = \frac{U_m I_m}{2} \cos(2\pi(2f)t - \varphi) + \frac{U_m I_m}{2} \cos(\varphi) + \sum_{k=1}^{\infty} \left\{ \begin{aligned} & \frac{U_m I_{ecc}, k_1}{2} \cos(2\pi(2f - kf_r)t - \alpha_1) \\ & + \frac{U_m I_{ecc}, k_1}{2} \cos(2\pi(kf_r)t + \varphi_1) + \\ & \frac{U_m I_{ecc}, k_2}{2} \cos(2\pi(2f + kf_r)t - \alpha_2) \\ & + \frac{U_m I_{ecc}, k_2}{2} \cos(2\pi(kf_r)t + \varphi_2) \end{aligned} \right\} \quad (18)$$

Where α_1 and α_2 are the initial phase angle at a frequency $f+kf_r$ and $f-kf_r$ respectively.

It can be seen, that the instantaneous power contains a dc level and additional components at f_r frequency.

Now if we take into account the magnetic saturation, the saturation characteristic components at f_{sat} appear in the stator current [7].

$$(19) \quad f_{sat} = ((k.n_b \pm n_d) \cdot \frac{(1-s)}{p} \pm 2.n_{sat} \pm \vartheta) f$$

where, p is pole number, n_b is number of rotor bars, ϑ is harmonic order ($\vartheta = \pm 1, \pm 3, \dots$), $n_d = 0$ (for healthy motor) and $n_d = 1, 2, \dots$ (For faulty motor), n_{sat} is saturation ($n_{sat} = \pm 1, \pm 2, \dots$) and s is the slip.

These saturation characteristics (fundamental, principal rotor slot and mixed eccentricity fault), are added to the instantaneous power spectrum components.

Diagnosis of Mixed Eccentricity for Saturated Squirrel Induction Motor Simulation results

A software is developed to solve the various differential equations by employing the fourth order Runge-Kutta technique, this for the study of the SCIM behaviour for the case of a healthy and mixed eccentricity faulty motor, with and without the saturation conditions. Simulations confirm the advantages of the IPS technique (the parameters of SCIM are presented in appendix).

For the case of the healthy motor loaded with a constant torque, the instantaneous power spectrum without and with saturation including the fundamental component 100Hz and principal rotor slot harmonics (PSH₁, PSH₂ and PSH₃), are shown in Figure 1 and Figure 2 respectively.

Figure 2 shows, that the low and up, saturation harmonics (SHL and SHU) are in the neighbourhood of the principal rotor slot harmonics (PSH₁ and PSH₃).

For the case of the faulty motor (by introduction of the mixed eccentricity fault), the Figures 3 and 4 show the IPS with and without saturation. The results show also that without saturation effect, the mixed eccentricity harmonics Low and Up (MEL and MEU) are sided band, in the neighbourhood of the PSH₁ and PSH₂ (Figure 3). On the other hand the effect of saturation seems very well by the presence of the harmonics of saturation on both sides the harmonics of eccentricity faults (Figure 4).

Experimental results

Figure 5 illustrates experimental system scheme to detect faulty conditions. This bench includes two 3-phase squirrel cage induction motors, 4 kW, 1500 rpm, rated supplied 380

V, 50 Hz, coupled to a permanent magnet synchronous generator. One of the motors is the healthy machine and the other is the faulty machine with mixed eccentricity of the squirrel cage. The synchronous generator is connected to a variable resistive load. Figure 6 shows the implemented test bench.

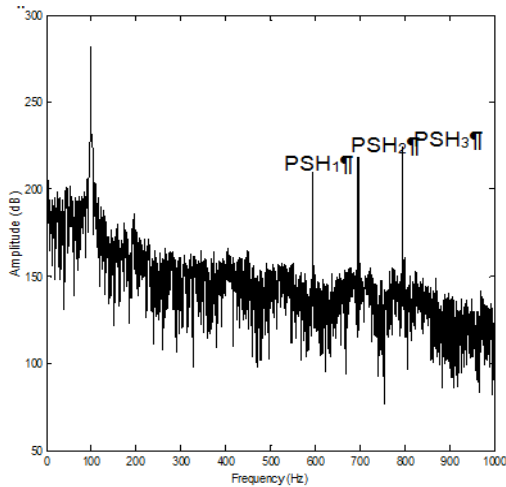


Fig.1. IPS for healthy motor and without saturation

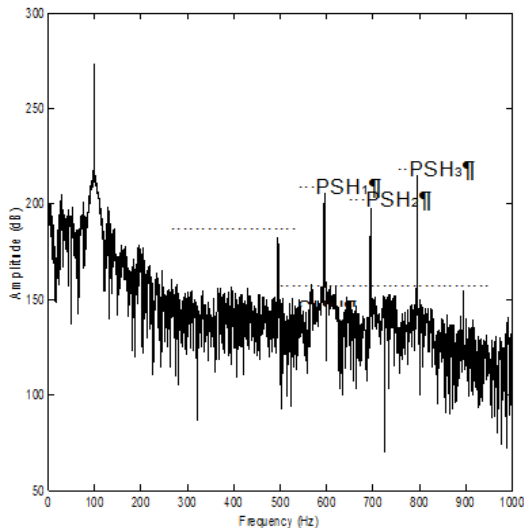


Fig.2. IPS for healthy motor and with saturation

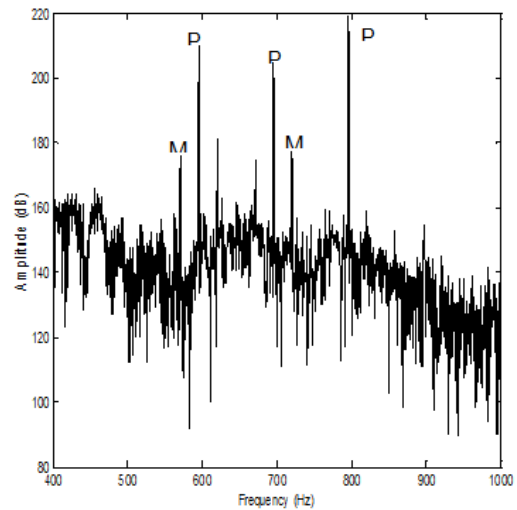


Fig.3. IPS for 30% Mixed Eccentricity and without saturation

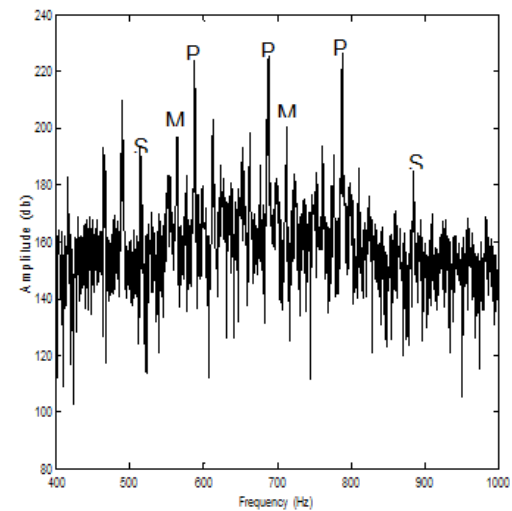


Fig.4. IPS for 30% Mixed Eccentricity and with saturation.

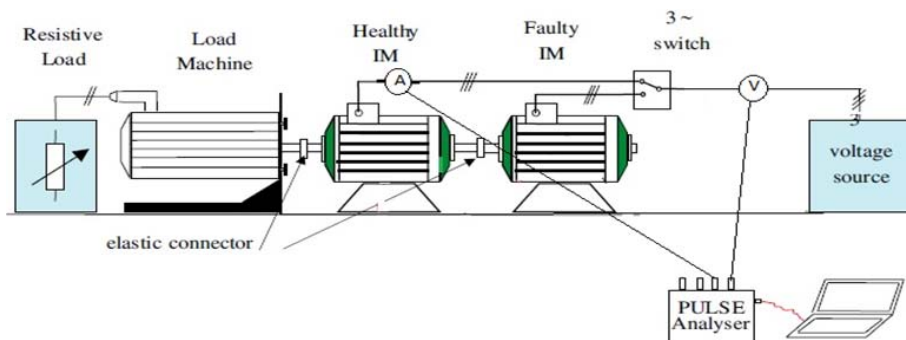


Fig.5. Detection system scheme

Figure 7 shows the no-load characteristic of the machine in order to obtain the saturation factor for the machine under different values of the applied voltages, it can be concluded that for the rated voltage machine is in the saturated region with the saturation factor $k_{gsat} = U_{nonsat}/U_{sat} = 1.2$.

Instantaneous power signature analysis of the healthy

motor is shown in the Figure 8. It can be noticed, that both practical and simulation spectrum results are comparable (the principal harmonics components can be identified at 100 Hz).

Figure 9 shows the instantaneous power spectrum for faulty motor without saturation. The Low and Up mixed eccentricity harmonics (MEL and MEU) are sided band,

and detected in the neighbourhood of the principal slot harmonics, this confirms the simulation results (Figure 3).

For the case of the faulty motor with saturation (Figure 10), the mixed eccentricity harmonics are in the proximity of the saturation harmonic position, which also confirms the simulation results.

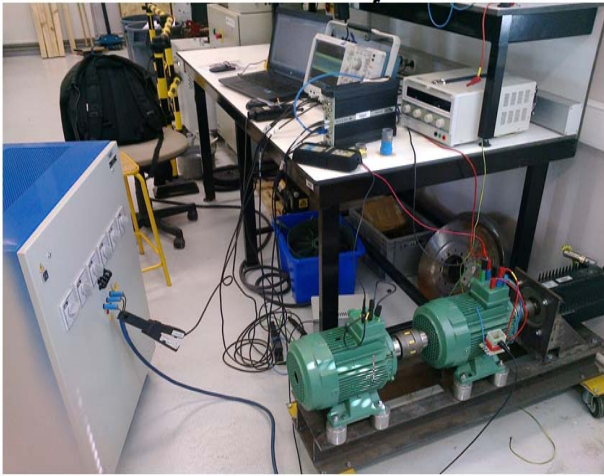


Fig.6. Experimental bench test

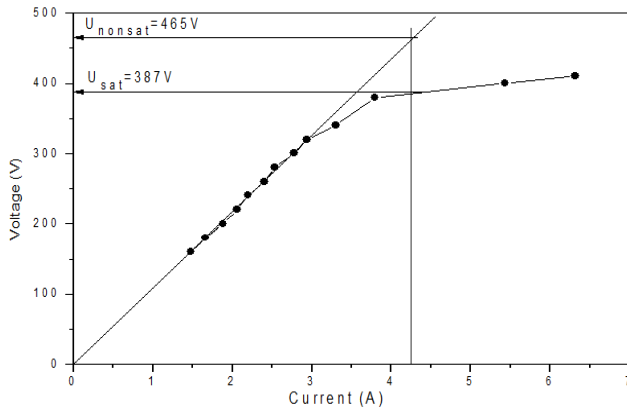


Fig.7. No-load characteristic of the experimental motor. Saturation factor for rated voltage $k_{gsat} = 1.2$

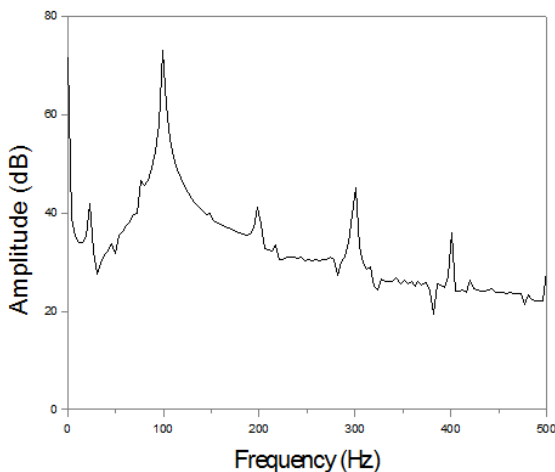


Fig.8. IPS for healthy motor (experimental result).

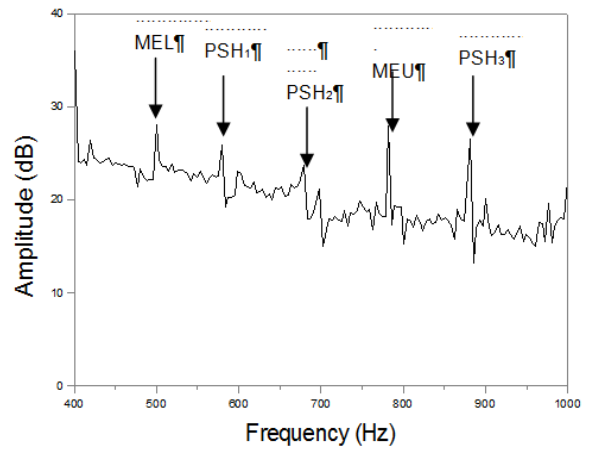


Fig.9. IPS for faulty motor and without saturation at full load (experimental result).

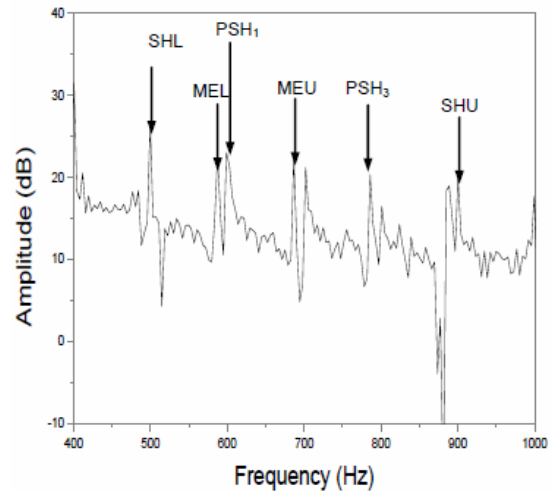


Fig. 10. IPS for faulty motor and with saturation at full load (experimental result).

Conclusion

This paper presents a non-invasive method for detection of mixed eccentricity fault in saturated squirrel cage induction motor, using instantaneous power spectrum. The advantages of the proposed method compared to the others methods, are, the simplicity to implement, and to interpret, and the low cost of the set-up. It showed in the health case that the saturation harmonic is present in the neighbourhood of the PSH in agreement with the experimental results.

Likewise, simulation results shown, that the magnitude and the position of the saturation harmonic in the neighbourhood of the mixed eccentricity harmonics, will contribute in the fault motor diagnostic technique. Finally, the experimental tests realized in different operation forms of induction machine confirm our results obtained in [7].

Appendix

Machine Parameters: 7.5 Hp, 36 stator slots, 28 rotor bars,

$R_s = 3.5332$	Ω	stator resistance
$L_s = 0.028$	H	stator inductance
$L_r = 0.28$	μH	rotor inductance
$R_r = 68.34$	$\mu\Omega$	rotor resistance
$J = 0.02$	kg.m^2	rotor inertia

Authors: Dr Chaouch Abdellah, University of Mostaganem Faculty of Sciences and Technology, Mostaganem, Algeria, E-mail: ikchaouchdz@yahoo.fr ;
prof. Bendiabdellah Azeddine, University of Sciences and Technology of Oran, Faculty of Electrical Engineering, Oran, Algeria.
Remus Pusca, Raphael Romary and Jean Philippe Lecointe, Electrotechnical and Environment Systems Laboratory (EESL), Artois University, Technoparc Futura, Bethune 62400, French

REFERENCES

- [1] Georgakopoulos I.P, Mitronikas E.D, Safacas A.N. Detection of Induction Motor Fault in Inverter Drives Using Inverter Input Current Analysis. IEEE Trans Ind Electronics 2011; 58: 4365-4373.
- [2] Bonnett A. H, Soukup G. C. Cause and Analysis of Stator and Rotor Failures in Three-Phase Squirrel-Cage Induction Motors. IEEE Trans Ind Appl 1992; 28; 4: 921-937.
- [3] Braham A, Lachiri Z. Diagnosis of Broken Bar Fault in Induction Machines Using Advanced Digital Signal Processing. IREE 2010; 5: 1460-1468.
- [4] Laribi S, Bendiabdellah A. Stator Short Circuit And Broken Bar Faults Diagnosis Of An Indirect Vector Control Squirrel Cage Induction Motor. IREE 2010; 5: 2088-2094.
- [5] Siddique A, Yadava G. S. A Review of Stator Fault Monitoring Techniques of Induction Motors. IEEE Trans Energy Conversion 2005; 20; 1: 106-114.
- [6] Bachir S, Tnani S, Trigeassou J. C, Champenois G. Diagnosis by Parameter Estimation of Stator and Rotor Faults Occurring in Induction Machines. IEEE Trans Ind Electron 2006; 53; 3: 963-973.
- [7] Chaouch A, Bendiabdellah A, Mixed Eccentricity Fault Diagnosis in Saturated Squirrel Cage Induction Motor. International Review on Modelling and Simulations (IREMOS), vol. 5, No.3, June 2012.
- [8] Drif M, Benouzza N, Bendiabdellah A, Dente J.A. The use of instantaneous power spectrum in the detection of rotor cage faults on 3-Phase induction motors. ELECO 1999; International conference on electrical and electronics engineering: 351-355.
- [9] Stanislaw F. L, Sadrul Ula A .H. M, Trzynadlowski A. M. Instantaneous Power as a Medium for the Signature Analysis of Induction Motors. IEEE Trans Ind Appl 1996; 32; 4: 904-909.
- [10] Mamchur D. An instantaneous power spectra analysis as a method for induction motors fault detection. Proceedings of OWD 2011; 22-25 October 2011; Wisla: 407-412.